Journal of Zhejiang University-SCIENCE A (Applied Physics & Engineering)
ISSN 1673-565X (Print); ISSN 1862-1775 (Online)
www.zju.edu.cn/jzus; www.springerlink.com
E-mail: jzus@zju.edu.cn

High-efficiency technique based on dielectrophoresis for assembling metal, semiconductor, and polymer nanorods*

Heng YUAN[1], Kyu-jin KIM[1], Won-seok KANG[2], Byoung-ho KANG[1],
Se-hyuk YEOM[1], Jae-ho KIM[2], Shin-won KANG†‡[3]

([1]*School of Electrical Engineering and Computer Science, Kyungpook National University, 1370 Sankyuk-dong, Bukgu, Daegu 702-701, Korea*)
([2]*Department of Molecular Science and Technology, Ajou University, San 5, Woncheon-dong, Yeongtong-gu, Suwon 443-749, Korea*)
([3]*School of Electronic Engineering, College of IT Engineering, Kyungpook National University, 1370 Sankyuk-dong, Bukgu, Daegu 702-701, Korea*)
†E-mail: swkang@knu.ac.kr

Received May 18, 2010; Revision accepted Sept. 14, 2010; Crosschecked Dec. 10, 2010; Published online Jan. 18, 2011

Abstract: This paper presents a high-efficiency technique based on dielectrophoresis (DEP) for assembling metal, semiconductor, and polymer nanorods, which are synthesized by electrochemical deposition (ECD). The assembly patterns of these nanorods (width: 20 nm; length: 7 μm) were designed using a finite element method (FEM) simulation tool. Further, these nanorods were used in our experiment after their assembly patterns were fabricated. The assembly yield was found to be approximately 70% at an AC voltage of 30 $V_{p\text{-}p}$ and at frequencies of 20 and 30 kHz, and the DC voltage prevented the random alignment of the nanorods at the edge of the assembly pattern. Moreover, the above-mentioned nanorods, which had different permittivities, were found to have similar assembly yields. The proposed method can be improved and applied to nanostructure device fabrication.

Key words: Nanorod, Assembly, Dielectrophoresis (DEP), Finite element method (FEM), Electrochemical deposition (ECD) method
doi:10.1631/jzus.A1000231 **Document code:** A **CLC number:** O646

1 Introduction

In recent years, nanoscience and nanotechnology have been extensively researched in fields such as materials science, chemistry, mechanics, biology, and medicine. Nanostructures exhibiting novel properties due to a quantum confinement effect (Brus, 1983), such as nanoparticles (Wang *et al*., 2007), nanotubes (Spitalsky *et al*., 2010), nanowires (Xia *et al*., 2010), nanorods (He *et al*., 2010), and nanopores (Madampage *et al*., 2010), have been studied and used in various fields.

An assembly technique used to arrange nanorods at user-defined positions is necessary for the fabrication of nanodevices consisting of nanorods. Nanorods synthesized by electrochemical deposition (ECD) (Wirtz and Martin, 2003), in particular, are generally dispersed in a liquid medium after they are synthesized. Therefore, it is essential to develop a technique to assemble nanorods. Dielectrophoresis (DEP) has been widely used for carbon nanotube (CNT) assembly (Inoue *et al*., 2010) and selective DNA separation (Yokokawa *et al*., 2010). However, it is difficult to assemble high-density nanorods such as gold (Au) nanorods, owing to the fact that these nanorods cohere with each other because of the surface tension generated when they are dispersed in a solvent.

In this study, we synthesized three types of nanorods—metal, semiconductor, and polymer

‡ Corresponding author
* Project supported by the Basic Research Program of the Korea Science & Engineering Foundation (No. R0120060001027202006), and the Basic Science Research Program through the National Research Foundation of Korea (No. 2010-0001882)

nanorods. Then, we designed the assembly patterns of these nanorods after carrying out electric field simulations. We also evaluated the assembly performance of these nanorods. After fabricating the assembly patterns, we performed nanorod assembly experiments and compared the results.

2 Principle of dielectrophoresis

According to the principle of DEP, an additional force acts on a particle when a heterogeneous electric field is applied to the particle. The dielectrophoretic force and the moving direction are determined on the basis of the strength of the electric field, frequency of the source, size and shape of the particle, and permittivities of the particle and medium (Jones and Kallio, 1979). The dielectrophoretic force acting on a particle in an electric field is given as (Pethig, 1996)

$$F_{\mathrm{DEP}} = \Gamma \cdot \varepsilon_{\mathrm{m}} \mathrm{Re}[K(\omega)] \nabla |E|^2, \qquad (1)$$

where Γ is the geometry coefficient, $K(\omega)$ is the Clausius-Mossotti factor, and $\nabla|E|^2$ is the gradient of the energy density of the electric field. In the case of a cylindrical nanorod, Eq. (1) is rewritten as

$$F_{\mathrm{DEP}} = \frac{3\pi}{4} a^2 l \cdot \varepsilon_{\mathrm{m}} \mathrm{Re}\left[\frac{\varepsilon_{\mathrm{p}}^* - \varepsilon_{\mathrm{m}}^*}{\varepsilon_{\mathrm{p}}^* + 2\varepsilon_{\mathrm{m}}^*}\right] \nabla |E|^2, \qquad (2)$$

where a is the radius of nanorods' section, l is the length of nanorods, ε_{p} and ε_{m} are the permittivities of the nanorod and medium, respectively. According to the principle of DEP, if the real part of the Clausius-Mossotti factor $\mathrm{Re}[K(\omega)]>0$, the nanorod can move to a region that has positive dielectrophoresis (pDEP), and if $\mathrm{Re}[K(\omega)]<0$, the nanorod can move to a region with negative dielectrophoresis (nDEP). A schematic of the nanorod assembly fabricated by DEP is shown in Fig. 1. This figure shows that a nonuniform electric field is formed between two electrodes. It also shows that a DEP force acts on the nanorod.

3 Experiments and results

3.1 Nanorod synthesis

The nanorods used in the experiment were synthesized using an anodic aluminum oxide (AAO) template (Anodisc$^{13\mathrm{TM}}$, Whatman Inc., USA) by ECD. Anodisc$^{13\mathrm{TM}}$, which has a uniform pore size of approximately 200 nm, is usually used as a filter. The radius of the nanorods cannot be controlled if an AAO template is used. However, their length and type, such as a metal, a semiconductor, or a macromolecule, can be controlled, and we can also synthesize nanorods comprising several materials with varying compositions (Ag-Au-Ag, Ag-polypyrrole (PPY)-Au, etc.).

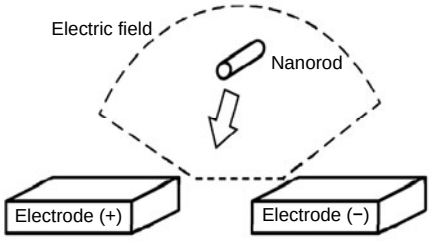

Fig. 1 Schematic diagram of nanorod assembly by the dielectrophoresis

First, an Ag layer (70-nm or 100-nm thick) was deposited on one side of the AAO template, which was used as the working electrode. A Pt wire and an Ag/AgCl electrode were used as the counter electrode and the reference electrode, respectively. Then Ag nanorods were synthesized using an Ag-plating solution (Technic Silver 1025, Technic Inc., USA) at −800 mV for 1 C (10 min). Au nanorods were synthesized using an Au-plating solution (Orotemp 24 Gold Salts, Technic Inc., USA) at −850 mV for 7 C (7 h). After that, the template was immersed in HNO_3 solution (90%, v/v) for 1 h to melt the Ag layer. Then the template was dissolved by immersion in 3 mol/L NaOH for approximately 5 h. After the synthesized nanorods were centrifuged and rinsed several times, they were suspended in an aliquot of EtOH.

Polymer nanorods were synthesized by electropolymerization using a plating solution (0.1 mol/L pyrrole, and 0.1 mol/L tetraethylammonium tetrafluoroborate in acetonitrile) at ±900 mV for 2.5 C (30 min). CdSe nanorods were fabricated by a cyclic voltammetry (CV) method and then electrodeposited using a plating solution (0.25 mol/L sulfuric acid, 0.03 mol/L cadmium sulfate, and 0.7 mmol/L selenium dioxide in deionized water) by sweeping the voltage between −350 and −800 mV (20 h). These nanorods were deposited layer by layer in the pores of the AAO template for 56000 cycles. Fig. 2 shows the synthesis process of Au nanorods. The synthesis

processes of the PPY and CdSe nanorods were similar to that of Au nanorods.

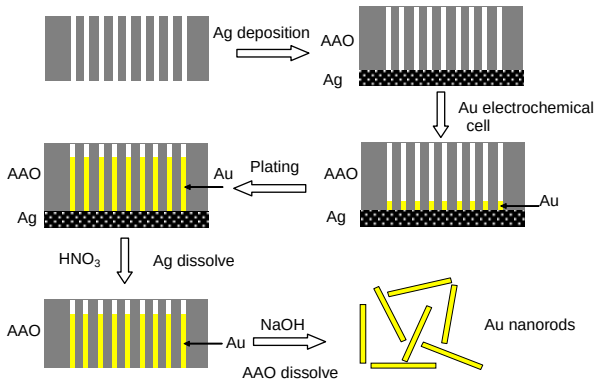

Fig. 2 Schematic process of Au nanorods

The growth rate of each type of nanorod based on the induced charge is shown in Fig. 3. The growth rate of the CdSe nanorods is not very high, because these nanorods are synthesized by the CV method.

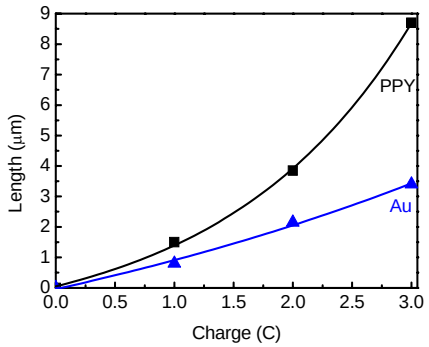

Fig. 3 Growth rate of Au and polypyrrole (PPY) nanorods

CdSe nanorods are not described because they are synthesized by cycle voltammetry

The nanorods used in the assembly experiment were 7-μm long and 200-nm wide. The scanning electron microscope (SEM) image of the synthesized Au nanorods is shown in Fig. 4.

3.2 Assembly simulation and fabrication

On the basis of the DEP principle, ANSYS^{TM}, a well-known finite element method (FEM) simulation tool, was used to design and optimize the nanorod assembly prior to carrying out the nanorod assembly experiment. First, on the basis of the assumption that the assembly pattern of the nanorod was made of Au, assembly simulation was carried out for optimizing the gap between the assembly patterns (where the nanorods were assembled). Chloroform was used as the media solution to preserve the nanorods. The side view of simulation result of the DEP acting on a nanorod is shown in Fig. 5.

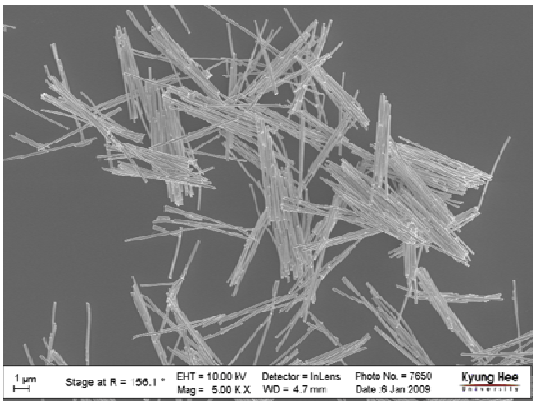

Fig. 4 SEM image of the synthesized Au nanorods

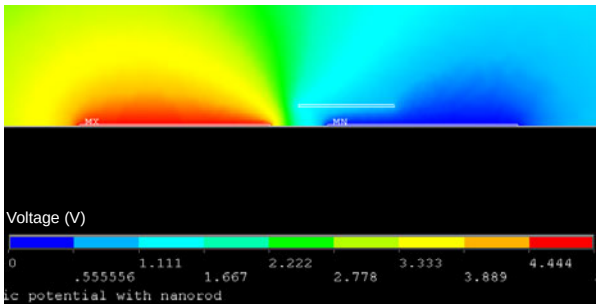

Fig. 5 Side view of simulation result of DEP acting on a nanorod

Voltages of +5 V and 0 V were applied to the left and right electrodes, respectively (Fig. 5). The simulation result shows that the electric field bends around the nanorods. The nanorod assembly pattern was designed after the nanorod assembly was optimized. The assembly pattern of the synthesized nanorods is shown in Fig. 6a. We supplied voltages of +5 V and 0 V to the first and second electrodes, respectively. The simulation result is shown in Fig. 6b.

As shown in Fig. 6, the result shows that the electric field is concentrated at certain sites, and the field strength is minimum at the edge of the electrode where the angle α is equal to 45°.

Then, from the simulation results, the assembly patterns of the nanorods were fabricated using a conventional lift-off process. First, an oxide layer (1000-nm thick) was grown on a p-type silicon wafer

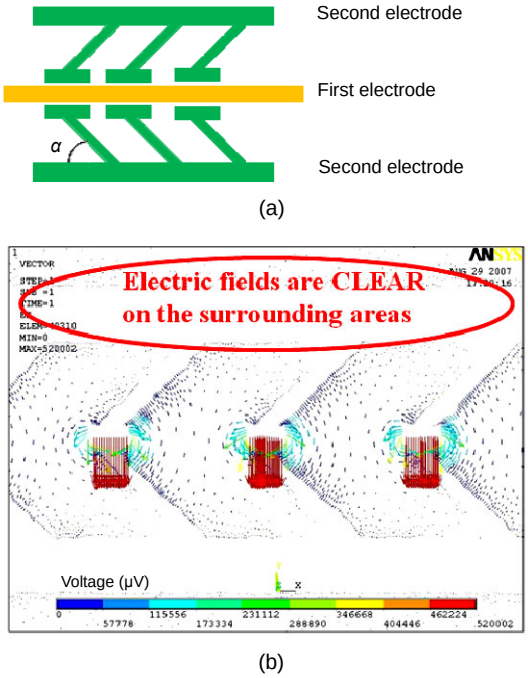

Fig. 6 Schematic (a) and electric field (b) simulations of the proposed nanorod assembly electrode

by wet thermal oxidation to prevent current leakage. After patterning the photoresist using AZ 5214, a Ni layer (15-nm thick) and an Au layer (135-nm thick) were deposited on the wafer using e-beam evaporation. The photoresist was then removed using acetone. Finally, a Si_3N_4 layer (150-nm thick) was deposited on the electrode to isolate the nanorods from the electrodes. The gap between AC and DC electrodes of the fabricated electrode assembly is approximately 5 μm.

3.3 Nanorod assembly experiments

The nanorod assembly system used in this study is shown in Fig. 7. This system consists of a probe station, a function generator, a microscope, a lamp, a charge coupled device (CCD) camera, and a PC. After fixing the fabricated nanorod assembly at the center of the probe station, power was supplied to the nanorods through the probe station from the function generator. The experimental assembly results can be observed on the PC.

The nanorod assembly experiment was performed to verify the simulation results. The microscope images of the nanorods array which under the condition of 20 $V_{p\text{-}p}$, 20 kHz (AC) and 10 V (DC) are shown in Figs. 8a and 8b, respectively.

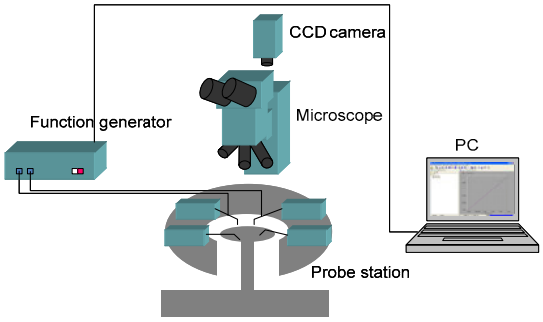

Fig. 7 Schematic of nanorod assembly system

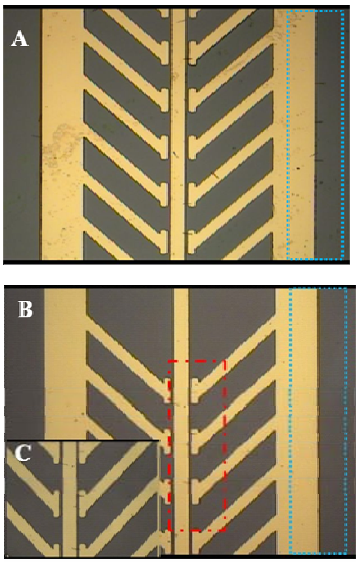

Fig. 8 Optical microscope images obtained after nanorod assembly

(a) Without applying DC voltage (AC of 20 $V_{p\text{-}p}$, 20 kHz); (b) Applying a DC voltage of 10 V; (c) Scale-up image of the left box of (b). The right box of (b) denotes the random placement of the nanorods at the edge of the electrode

Figs. 8a and 8b show that the nanorods were accurately aligned with the application of the DC voltage as compared to that without the DC voltage. Moreover, the DC electrode could prevent the random alignment of the nanorods at the edge of the electrodes. This result is in good agreement with the simulation result. The SEM image of the assembled Au nanorod is shown in Fig. 9. An Au nanorod is assembled in the gap between the two electrodes (up and down blocks).

To evaluate the assembly performance of the proposed electrode, three types of nanorods—metal (gold), polymer (PPY), and semiconductor (CdSe) nanorods—having different permittivities were used in the nanorod assembly experiment, because the

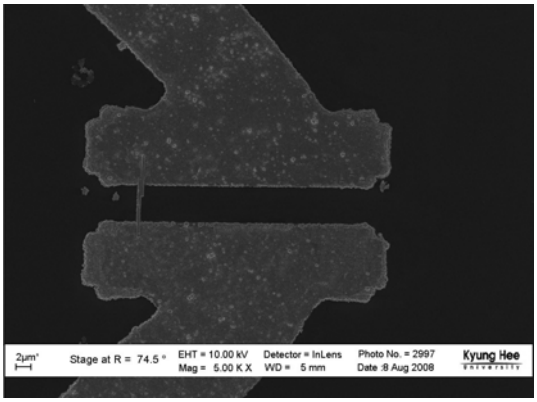

Fig. 9 SEM image of nanorod assembly

permittivity of the nanorods as well as that of the medium affects the dielectrophoretic force. The assembly experiment was performed by applying an AC voltage of 30 $V_{p\text{-}p}$ at frequencies ranging from 10 kHz to 1 GHz at the AC electrode and a DC voltage of 10 V at the DC electrode (Fig. 10).

Fig. 10a shows a plot of the assembly yield against frequency. The assembly yield was the highest, i.e., 70.8%, at frequencies of 20 and 30 kHz, and it gradually decreased above 30 kHz. The assembly yield was less than 20% below 10 kHz. In (Inoue *et al*., 2010), the assembly performance of CNTs or nanowires synthesized by DEP has been reported to be high when the frequency applied was around several gigahertz. However, in our experiment, the assembly yield was the highest at around 20 and 30 kHz.

The assembly performances of nanorods made of various materials are shown in Fig. 10a. The figure shows that the assembly yields of metal, polymer, and semiconductor nanorods are similar and tend to decrease above 30 kHz. It is assumed that since the nanorods used in our experiment have a high density, the low frequency at the assembly electrode could have resulted in slow movement of the nanorod and high assembly yield. The similar assembly yield of the three types of nanorods suggests that the permittivity of the medium, ε_m, and not the permittivity of the nanorods as indicated by Eq. (2), is a dominant factor, because the nanorods used in our experiment have a high density and a large size. Fig. 10b shows a plot of the AC amplitude against the assembly yield. The frequency was fixed at 30 kHz, and a small DC offset was induced at the DC electrode, which reduced the effect of the DC electrode. The assembly yield increased with the amplitude, as predicted by the DEP principle.

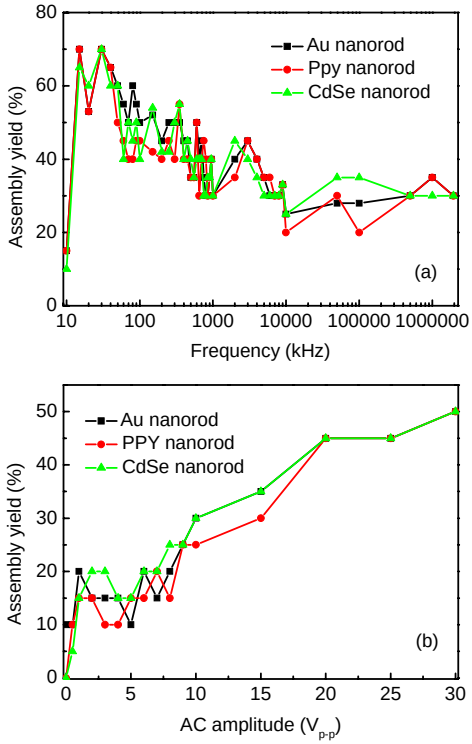

Fig. 10 Plot of assembly yield against (a) induced frequency on the AC electrode (at an amplitude of 30 $V_{p\text{-}p}$ and a DC voltage of 10 V) and (b) AC amplitude on the DC electrode (at a frequency of 30 kHz)

4 Conclusions

This paper presented a high-efficiency nanorod assembly technique based on DEP. The assembly electrode was designed after carrying out electric field simulations. The nanorod assembly yield was measured under different frequencies and amplitude conditions of the applied voltage. Further, a nanorod assembly experiment was performed using not only the polymer and semiconductor nanorods but also metal nanorods, which are difficult to assemble.

The assembly yield obtained using our assembly pattern was 70.8% at frequencies of 20 and 30 kHz and at an AC voltage of 30 $V_{p\text{-}p}$. Furthermore, the assembly yields of the three types of nanorods were similar. The proposed assembly pattern can be used for the fabrication of nanorod arrays and the development of measurement kits for nanorods and nanowires made of novel materials.

References

Brus, L.E., 1983. A simple model for the ionization potential, electron affinity, and aqueous redox potentials of small semiconductor crystallites. *The Journal of Chemical Physics*, **79**(11):5566-5571. [doi:10.1063/1.445676]

He, Z.Y., Li, Y.G., Zhang, Q.H., Wang, H.Z., 2010. Capillary microchannel-based microreactors with highly durable ZnO/IiO_2 nanorod arrays for rapid, high efficiency and continuous-flow photocatalysis. *Applied Catalysis B: Environmental*, **93**(3-4):376-382. [doi:10.1016/j.apcatb.2009.10.011]

Inoue, K., Wanagisawa, R., Koike, E., Nishikawa, M., Takano, H., 2010. Repeated pulmonary exposure to single-walled carbon nanotubes exacerbates allergic inflammation of the airway: Possible role of oxidative stress. *Free Radical Biology and Medicine*, **48**(7):924-934. [doi:10.1016/j.freeadbiomed.2010.01.013]

Jones, T.B., Kallio, G.A., 1979. Dielectrophoretic levitation of spheres and shells. *Journal of Electrostatics*, **6**(3):207-224. [doi:10.1016/0304-3886(79)90092-5]

Madampage, C.A., Andrievskaia, O., Lee, J.S., 2010. Nanopore detection of antibody prion interactions. *Analytical Biochemistry*, **396**(1):36-41. [doi:10.1016/j.ab.2009.08.028]

Pethig, R., 1996. Dielectrophoresis: Using inhomogeneous AC electrical fields to separate and manipulate cells. *Critical Reviews in Biotechnology*, **16**(4):331-348. [doi:10.3109/07388559609147425]

Spitalsky, Z., Tasis, D., Papagelis, K.K., Galiotis, C., 2010. Carbon nanotube—polymer composites: Chemistry, processing, mechanical and electrical properties. *Progress in Polymer Science*, **35**(3):357-401. [doi:10.1016/j.progpolymsci.2009.09.003]

Wang, C.Z., Xiao, X.G., Hu, H.Q., Rong, Y.H., Hsu, T.Y., 2007. Nanoparticle morphology in FeNi-Cu granular films with giant magnetoresistance. *Physica B: Condensed Matter*, **392**(1):72-78. [doi:10.1016/j.physb.2006.11.001]

Wirtz, M., Martin, C.R., 2003. Template-fabricated gold nanowires and nanotubes. *Advanced Materials*, **15**(5):455-458. [doi:10.1002/adma.200390106]

Xia, X.H., Tu, J.P., Zhang, J., Xiang, J.Y., Wang, X.L., Zhao, X.B., 2010. Fast electrochromic properties of self-supported Co_3O_4 nanowire array film. *Solar Energy Materials and Solar Cells*, **94**(2):386-389. [doi:10.1016/j.solmat.2009.08.020]

Yokokawa, R., Manta, Y., Namura, M., Takizawa, Y., Le, N.C.H., Sugiyama, S., 2010. Individual evaluation of DEP, EP and AC-EOF effects on λDNA molecules in a DNA concentrator. *Sensors and Actuators B: Chemical*, **143**(2):769-775. [doi:10.1016/j.snb.2009.10.025]